Reliable heatwave attribution based on successful operational weather forecasts

Nicholas Leach (nicholas.leach@physics.ox.ac.uk)
University of Oxford https://orcid.org/0000-0003-4470-1813

Christopher Roberts
European Centre for Medium-Range Weather Forecasts

Daniel Heathcote
University of Bristol

Dann Mitchell
University of Bristol https://orcid.org/0000-0002-0117-3486

Vikki Thompson
University of Bristol

Tim Palmer
University of Oxford https://orcid.org/0000-0002-7121-2196

Antje Weisheimer
University of Oxford https://orcid.org/0000-0002-7231-6974

Myles Allen
University of Oxford https://orcid.org/0000-0002-1721-7172

Physical Sciences - Article

Keywords:

Posted Date: August 3rd, 2022

DOI: https://doi.org/10.21203/rs.3.rs-1868647/v1

Reliable heatwave attribution based on successful operational weather forecasts

Nicholas J. Leach,[1*] Christopher D. Roberts,[2] Daniel Heathcote,[1,3]
Dann M. Mitchell,[3] Vikki Thompson,[3] Tim Palmer,[1]
Antje Weisheimer,[1,2,4] Myles R. Allen,[1,5]

[1]Atmospheric, Oceanic, and Planetary Physics, Department of Physics,
University of Oxford, Oxford OX1 3PU, UK
[2]Earth System Predictability Section, Research Department,
European Centre for Medium-Range Weather Forecasts, Reading RG2 9AX, UK
[3]School of Geographical Sciences,
University of Bristol, Bristol BS8 1SS, UK
[4]National Centre for Atmospheric Science,
Atmospheric, Oceanic, and Planetary Physics, Department of Physics,
University of Oxford, Oxford OX1 3PU, UK
[5]Environmental Change Institute, School of Geography and the Environment,
University of Oxford, Oxford OX1 3QY, UK

[*]To whom correspondence should be addressed; E-mail: nicholas.leach@stx.ox.ac.uk.

Extreme weather attribution, quantifying the role of human influence in specific weather events, is of interest to scientists, adaptation planners and the general public[1]. However, the devastating 2021 Pacific Northwest heatwave challenged conventional statistical approaches to attribution due to the absence of similar events in the historical record, and model-based approaches due to poor representation of key causal processes in current climate models[2]. Here we use state-of-the-art operational medium-range and seasonal weather prediction systems, applied for the first time to this kind of climate question and unequivocally able to simulate the detailed physics of the heatwave in question, to show that human influence on the climate made this event at least 8 [2–30] times more likely to occur. Quantifying the absolute probability of such an unprecedented event is more challenging, but the length of the observational record suggests at least a multi-decade return-time in the current climate, with the likelihood doubling every 17 [10–50] years at the current rate of global warming. Our forecast-based approach synthesises the storyline approach, which examines human influence on the physical drivers of an event in a deterministic manner[3], and the probabilistic approach, which assesses how the frequency of a class of events has been affected by human influence[4]. If developed as a routine service in a number of forecasting centres, it could provide reliable estimates of the changing probabilities of all extreme events that can be represented in forecast models, which is critical to supporting effective adaptation planning[5,6].

Introduction

Although considerable progress has been made over the past decade in quantifying the impact of climate change on individual extreme weather events[4,1], challenges remain over the assessment of the most extreme events. Such events are particularly difficult to draw confident conclusions about due to the lack of historical analogues, and their often poor representation in the climate models normally used for event attribution. Two contrasting mainstream frameworks to event attribution have been developed: the storyline approach, which examines anthropogenic influence on the causal drivers of the extreme in question and is therefore highly conditioned on its specific characteristics[7,3,8]; and the probabilistic approach, which aims to determine how anthropogenic influence has affected the likelihood of events at least as extreme as the one in question[9,10].

A key challenge for extreme event attribution is that we cannot make direct observations of a world without human influence on the climate, so all approaches must involve some kind of modelling, either statistical[11] or dynamical[10]. Both face difficulties with the most extreme events, especially when considering the nonlinear processes that often drive unprecedented events. Statistical models used in conventional attribution can break down when faced with such events due to the lack of appropriately similar historical samples[12], while numerical climate models generally used in attribution studies are typically coarse (O(100km) horizontal resolution), and poorly represent important processes involved in the development of extreme weather events, such as blocking[13] and atmospheric rivers[14]. Even with a "perfect" model of the earth system, the unconditioned nature of the vast majority of climate model simulations used in attribution means that obtaining enough analogues of unprecedented events[15] to avoid the same issue faced by statistical modelling of the observational record requires very large ensembles, possibly beyond current computational limits[16]. Crucially, the role of climate change

in an individual event may differ from that in other events of the same class due to the specific physical processes behind it[17,18].

The storyline framework overcomes some of these issues, and the risk of a false negative, by examining the impact of climate change on the causal drivers of an event deterministically. For instance, one might separate out the thermodynamic (typically high confidence in response to climate change and well-represented in numerical models) and dynamic (typically much lower confidence in response to climate change, and more poorly represented in numerical models) drivers of an event, for example by conditioning on the concurrent large scale atmospheric circulation. One approach for applying such conditioning is to "nudge" climate model simulations towards the large-scale flow observed during a particular extreme[19,20]. The storyline approach does not, however, provide quantitative information about how climate change has affected the probability of the event in question, which is of interest to the general public and relevant to policymakers for adaptation planning.

We propose a forecast-based approach that could synthesise the probabilistic and storyline frameworks to extreme event attribution[21]. Although they belong to the same class of dynamical model and often share components[22], operational weather forecast models are typically run at much higher resolutions than climate models, improving their overall physical representation of extremes. They are validated for producing predictions that span the range of possible weather by the centres that produce them to a much higher degree than climate models, where other aspects are more important. In addition to this high level of explicit validation, using a model that has successfully predicted an event ensures that the model is able to accurately represent all the processes involved in the event in question, increasing the reliability of attribution statements based upon it[18]. Stepping back through lead times allows for a robust storyline-like framing by examining how climate change has affected the causal drivers of the specific event within the limits of predictability. Probabilistic attribution can be performed using a reliable forecast

ensemble, with the level of conditioning set by the lead time - the limiting case of long lead times is equivalent to a conventional unconditioned analysis. There has been some previous work into forecast-based attribution, using seasonal forecast models[23,24,25,26,27] and exploring the conceptual framework[28,29,30]. To our knowledge, however, this study is the first time that a complete forecast-based attribution has been carried out in a coupled operational forecast model at such a high resolution.

In this study we use the coupled operational ECMWF model (details in the Supplement) to analyse the Pacific Northwest heatwave, taking advantage of its successful predictions of this unprecedented event at leads of over a week. We perform counterfactual forecasts of the event by perturbing the initial and boundary conditions of the model in order to simulate how the heatwave might have emerged had it occurred in a cooler pre-industrial world, or a warmer future world. We then compare the counterfactual and operational forecasts to assess the impact of anthropogenic climate change on both the magnitude and probability-of-occurrence of the event. We believe that this forecast-based approach opens the door to not only a reliable and practical operational attribution system, but also to a robust way of generating projections of future weather explicitly referenced to the forecasts used already by adaptation planners[31].

The Pacific Northwest heatwave At the end of June 2021, a large fraction of the Pacific Northwest region of the US and Canada experienced unprecedented high temperatures, including the cities of Portland, Salem, Seattle and Vancouver (Figure 1). This heatwave (the "PNW heatwave") has been directly linked to many hundred excess deaths during and following it, making it the deadliest weather event on record for both Canada and Washington state[32]. The heatwave peak was observed between the 28th & 30th June, though temperatures were still exceptionally high on the days immediately before and after this period[33,34]. A large number of local maximum temperature records were broken during this period, including the Canadian

all-time record by a margin of 4.6 °C.

Based on current understanding, the heatwave arose from an optimal combination of proximal drivers[35,36,37,2]. Development of an omega block between the 23rd-27th coincided with the landfall of an atmospheric river (AR) on the 25th. Warm air was drawn up from the tropical West Pacific, heated diabatically through condensation in the river and then further heated adiabatically through subsidence: both the temperature and lapse rate at 500 hPa reached or approached record levels in the regions affected. This atmospheric heating was enhanced by soil moisture feedbacks[38] and high insolation at the land surface during the hottest hours of the day (Figure 2). Given the unprecedented nature of the observed heatwave, any dynamical numerical model would need to capture all these processes, including the coupling between them, in order to produce an accurate representation of the event.

Despite the observed temperatures lying far outside the historical record, the heatwave was well predicted by numerical weather forecast models such as from ECMWF at lead times of more than a week. The seasonal forecast from ECMWF captured one important aspect of the event: it predicted a thicker troposphere than average (measured by 500 hPa geopotential height) over the Pacific Northwest during the summer. A key change in the predictability of the exceptional temperatures occurred around June 21st, being the earliest point at which the penetration of the AR over land was well represented[37]. The success of these forecast models provides an opportunity to use them to examine the influence of anthropogenic climate change on the event as it actually occurred.

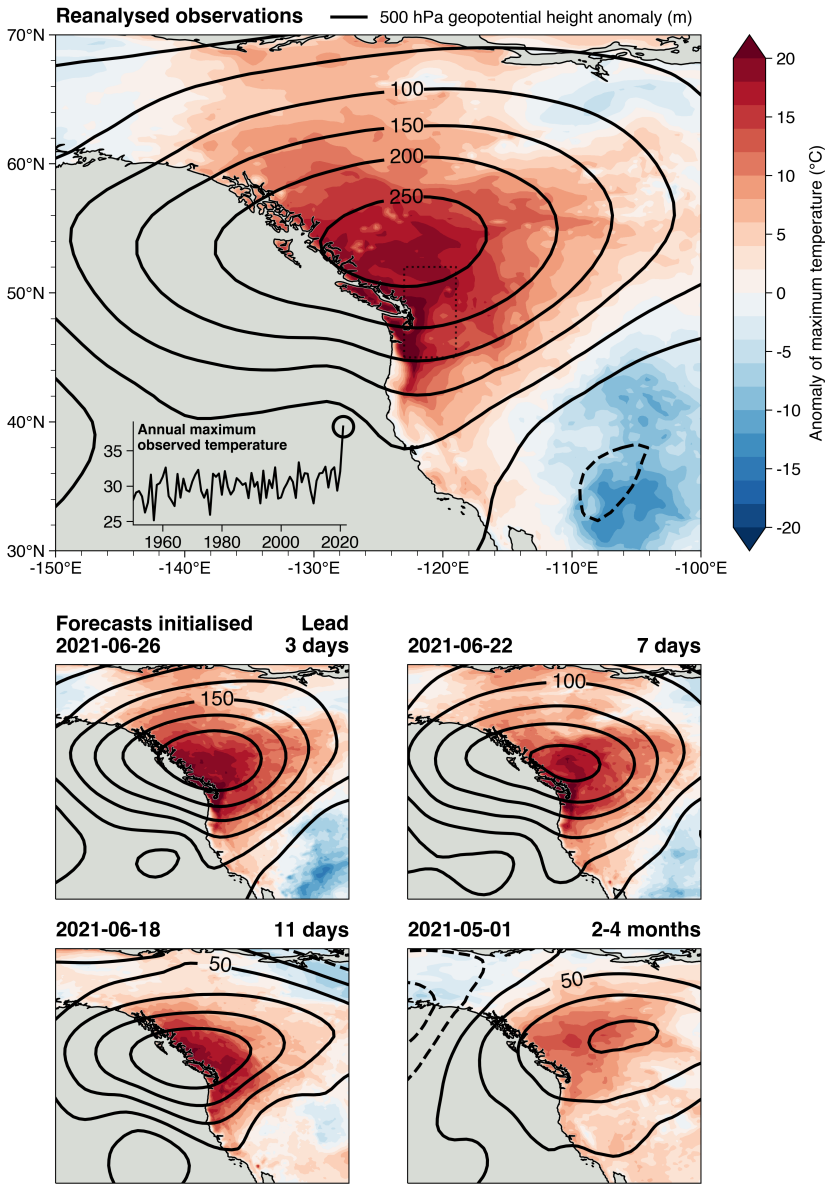

Figure 1: **Features and forecasts of the Pacific Northwest heatwave. Top panel:** Surface temperature anomalies at the time of the peak heat during the heatwave within the region enclosed by 45-52N, 119-123W (indicated by the dotted rectangle). Solid black contours show the 500 hPa geopotential height anomaly averaged over 26-30th June 2021. Data are from ERA5 reanalysis[39]. **Inset:** timeseries of annual maximum temperatures for the same dotted region. **Bottom panels:** As above, but taken from the ensemble member within the forecast initialised on the date given above each panel that predicted the nearest temperature to the reanalysis within the dotted region.

Forecast-based attribution

The date at which we initialise our perturbed forecasts is a key choice that allows us to condition our attribution analysis on different synoptic drivers of the heatwave, which become predictable at different leads[36,37]. The climate change response of drivers already present in the initial conditions is clearly not incorporated into our attribution results for each lead time due to this conditioning. Starting with the operational configurations of the ECMWF forecast model, we chose to focus on three medium-range and one seasonal forecast lead: 3 days, 7 days, 11 days and 2-4 months. These leads highlight the following aspects of the attribution:

- 3 days (2021-06-26): a forecast very highly conditioned on the synoptic drivers of the event, with several key drivers prescribed in the initial conditions, and the rest forecast near perfectly. At this lead, our experiments could be considered analogous to a storyline attribution framing.

- 7 days (2021-06-22): a highly conditioned forecast, with most simulated processes mirroring reality closely. However, the shape and gradient reversal magnitude of the block shows considerable variation in this ensemble.

- 11 days (2021-06-18, depicted in Figure 2): while the exceptional thickness of the tropospheric block was well predicted in a large proportion of the ensemble, the shape and associated gradient reversal was only captured in a few members. The occurrence of the AR was well predicted, but its location and penetration over land less so, with most members predicting a more southerly landfall. The low soil moisture and cloud cover was well captured by the majority of the ensemble.

- 2-4 months (2021-05-01): a considerably less conditioned forecast. For this lead, we take the peak heat event over the whole summer period since we do not expect the forecast

to predict the timing of the heatwave. Although the forecasts were unusually successful at predicting elevated geopotential height and temperatures over the summer in general, none of the peak heat events within individual ensemble members capture all of the detailed features of the PNW heatwave. At this lead, the ensemble can be viewed as being near-analogous to a high resolution unconditioned climate model simulation (though one that we know is able to represent the processes involved in the PNW heatwave accurately).

We then perturb the boundary and initial conditions of the operational forecast (technical details in the Supplement). First, we perturb the CO_2 concentrations in the atmosphere back to pre-industrial levels of 285 ppm, similar to[21]. Then we remove a balanced estimate of anthropogenic change between pre-industrial and the present-day in surface and sub-surface ocean temperatures, sea ice concentration, and sea ice thickness[40,41,42] from the initial state of the model. Perturbing the temperatures over the entire ocean depth means that we produce forecasts that are thermodynamically consistent with the changes in upper ocean heat content, in contrast to prescribed SST approaches[43,44]. We do not alter the land-surface, noting the high uncertainties in past trends for indicators such as soil moisture in this region[45,46,47]. Removing anthropogenic influence from the ocean state and reducing CO_2 levels produces a counterfactual "pre-industrial" forecast; we also apply identical perturbations in the opposite direction to produce a "future" forecast, in which the ocean state and CO_2 levels of 615 ppm correspond to approximately twice the level of global warming experienced at the present-day.

We find that despite the large impulse applied by the perturbed initial state upon forecast initialisation, the predictability of the heatwave is remarkably stable. The key synoptic drivers of the heatwave present in the original operational forecast remain intact. There are some changes consistent with the canonical response to global warming, including a thickening of the lower troposphere[48] and increased tropospheric water vapour[49] in the future forecast; and vice-versa in the pre-industrial forecast. As such, the perturbations have not altered the forecasts in such

a way that they produce "different" weather, and we can compare our forecasts to estimate the influence of anthropogenic global warming on the Pacific Northwest heatwave. This is consistent with[21], but is not guaranteed to be the case for every weather event.

This experiment design is consistent with the perturbed CO_2 experiments of[21] in another important respect: the adjustment to the new "pre-industrial" or "future" climate state occurs continually throughout the forecast. This adjustment typically means that as the lead time increases, the estimated attributable influence on the heatwave also increases. Interplay between dynamical noise and attributable signal in the forecasts, both of which increase with the lead time (short leads correspond to more confident but smaller attributable impacts and vice-versa) is discussed further in[21]. The adjustment means that any attributable impacts estimated directly from the forecasts are lower-bounds on the true anthropogenic impact. However, we find that attributable impacts on the heatwave are approximately linear with the coincidental global warming level within the perturbed forecasts across the range of leads explored (Supplementary Figure S7), consistent with[50]. Hence in addition to the impacts estimated directly from the perturbed forecasts, we also present impacts scaled to the global warming level within the forecast at the time of the heatwave.

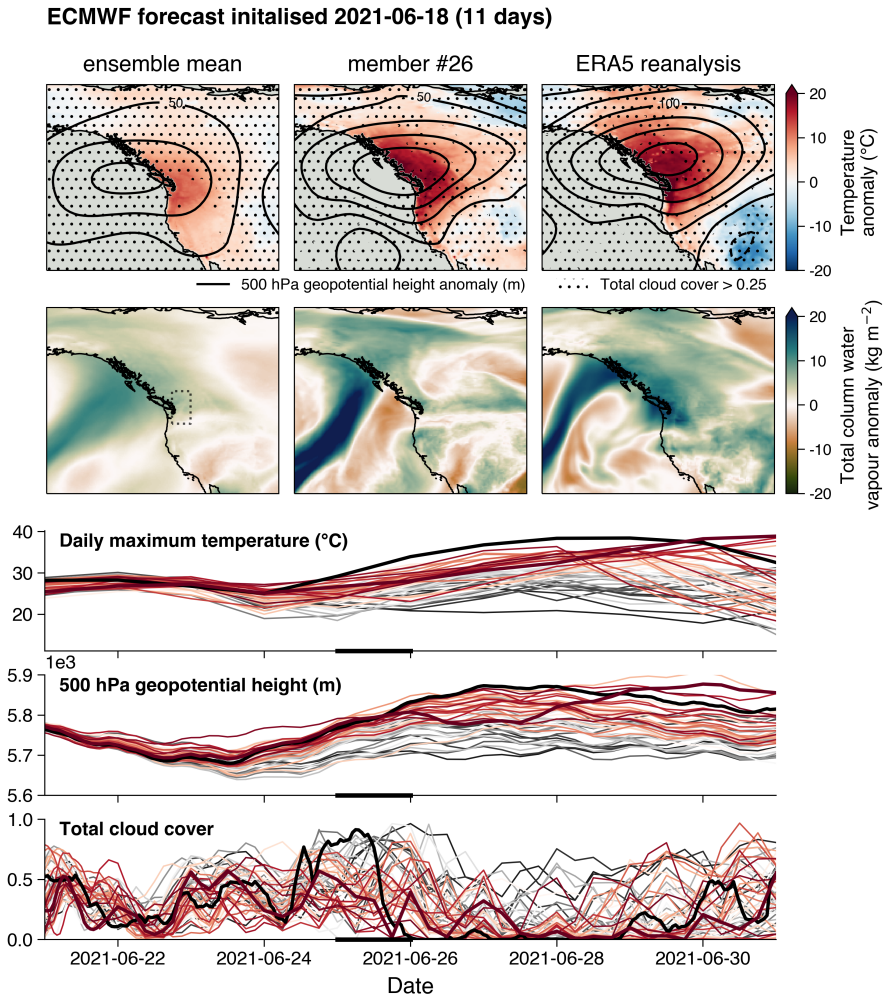

Figure 2: **Drivers of the PNW heatwave and their predictability in the forecast initialised 2021-06-18 (11 days). Top row:** temperature anomaly fields for the PNW heatwave in the ensemble mean, nearest member and reanalysis. Solid black contours indicate 500 hPa geopotential height anomalies and stippling indicates regions with total cloud cover greater than 25%. **Second row:** mean total column water vapour anomalies on the 25th June. The study region of 45-52N, 119-123W, over which fields are aggregated into timeseries, is indicated by the dotted rectangle. Anomalies shown are calculated relative to the 2001-2020 period. **Bottom three rows:** timeseries of daily maximum temperatures, total column water vapour and total cloud cover in each forecast ensemble member. The solid black line shows the reanalysis timeseries and the thick solid line shows the nearest member. The colour of each line indicates the rank of that ensemble member in terms of the peak temperature simulated during the heatwave period (dark grey = coolest, dark red = warmest). The solid black bar on the time axis of each panel indicates the averaging period used for the total column water vapour maps.

Results The results of our forecast-based approach can be presented either as the attributable human influence on the intensity of the heatwave or the probability of the heatwave. We find that the intensity of the heatwave is reduced in the pre-industrial forecasts for all lead times (Figure 3). Due to the continual adjustment of the forecasts to the initial condition perturbations, the attributable influence on the heatwave peak temperature, estimated as half the difference between the pre-industrial and future forecasts to maximise the signal to noise ratio, increases as the lead time increases, ranging from 0.28 °C [0.25 , 0.33][1] using the 3-day lead to 0.7 °C [0.35 , 1.0] using the seasonal forecast. We account for the continual adjustment of the perturbed forecasts by scaling the attributable influence by the ratio of the coinciding global land warming level to the observed present-day level of 1.6 °C[51]. This results in a best-estimate attributable impact on the heatwave intensity of 1.3 °C [0.5 , 1.9] for a current level of anthropogenic warming of 1.25 °C[52]. This accounts for approximately 20% of the 7 °C 2021 anomaly over previous annual maxima.

We quantify the attributable change in probability due to anthropogenic global warming using relative risk[53], estimating the probability of observing an extreme at least as extreme as the observed 2021 heatwave using an appropriate extreme-value or tail distribution, and then shifting this distribution by the attributable change in intensity for each lead time. As with the heatwave intensity, the relative risk tends to increase with forecast lead time due to the adjustment to the initial conditions. Our results are consistent with a linear relationship between log probabilities and the coinciding global land warming level. If we account for this adjustment by scaling log probabilities by the current global land warming level of 1.6 °C, we find a best-estimate relative risk of a factor of 8 times [2 , 30] considering all lead times, or analogously a fraction of attributable risk of 0.9 [0.5 , 0.97].

Using the current rate of global warming over land[52] we can further estimate that the proba-

[1]Numbers in square brackets represent a likely confidence range (17-83%).

bility of observing an event at least as warm as the 2021 Pacific Northwest heatwave is doubling every 17 [10 , 50] years, and will continue to do so unless the rate of global warming decreases. Given the length of the historical record and our estimated change in probability over this period, such an event would be associated with a multi-decade to multi-century return period at the present-day, thus making this doubling time very relevant for adaptation planning.

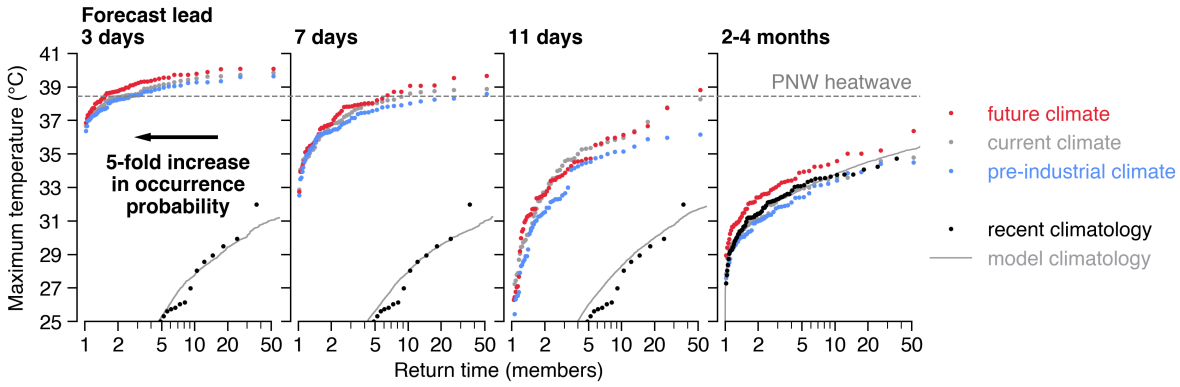

Figure 3: **Return-time diagram of the PNW heatwave in the operational and counterfactual forecast ensembles.** Each panel shows ensembles initialised at the lead given above the panel. Red, grey and blue dots indicate empirical return-time plots based on the ensemble members of the future, current and pre-industrial forecasts. The dashed grey line shows the temperature threshold observed during the PNW heatwave. The black dots indicate the recent climatology, based on detrended ERA5 reanalysis over 1950–2020. The solid grey line indicates the model climatology estimated using detrended hindcasts over 2001–2020 for the medium-range forecast, and using detrended and bias-corrected hindcasts over 1981–2020 for the seasonal forecast. The arrow in the left hand panel indicates, for illustration, the displacement along the log-scaled x-axis equivalent to a 5-fold increase in occurrence probability.

Discussion

The results presented here provide strong evidence of the impact of climate change on a specific extreme event, based on a model that has been demonstrated unequivocally to be able to simulate the event in question through a successful medium-range forecast. Our estimates of relative risk are lower than previous climate model-based estimates[54], albeit are not entirely incompatible within the context of the associated uncertainties and the fact that our estimates represent a lower bound on the impact of climate change on the heatwave (as was the case in[21]). The primary reason is that our model (unlike a typical climate model) is capable of simulating the multiple physical factors that contributed to the heatwave that occurred, so we are not relying on extrapolation of distributions from physically dissimilar events. Moreover, our imposed perturbations do not include the total sum of human influence on the climate. It is known that land surface feedbacks are important in the development of extreme heatwaves[55], and is plausible that if we had removed the influence of anthropogenic climate change from the initial land state in addition to the ocean state, the resulting attribution statement might have been stronger.

Nevertheless, we argue that the forecast-based methodology presented here represents an important advance in both attribution in general, and operational attribution. Rather than relying on multiple lines of evidence that would each be unsatisfactory in isolation, here we have presented a single adequate line. The key to the adequacy of the result is the ability of the model used to represent the event in question, demonstrated through successful prediction. This not only means that we have increased confidence in the model's response to external forcing[18,17], but also that the analysis is a genuine attribution of the specific event that occurred (rather than a mixture of events that share some characteristic like extreme temperatures, but differ in other important meteorological aspects). Forecast-based attribution provides many of the advantages of the storyline approach to attribution, but can still be used to provide quantitative estimates

of the changing probability of extreme events with climate change. The use of an operational weather forecast model demonstrates how this approach could be easily adapted to provide an operational system for attribution in real-time (or potentially even in advance[26]). Such a system would involve re-running operational forecasts with perturbed initial and boundary conditions as in the counterfactual forecasts we have presented here[56].

There remain a number of ways in which the forecast-based approach explored here could be further developed. Firstly, analysis of the forecasts would be simplified if they were started from balanced states, rather than continually adjusting to the new initial conditions throughout the forecast. This could be done by either including additional perturbations to the initial conditions (ie. to the land-surface and atmospheric states[26,57,56]), or possibly by perturbing the initial state using the operational data-assimilation itself. Secondly, while here we have chosen to use the exact setup used operationally by ECMWF, the uncertainty of forecast-based attribution statements could be reduced by increasing the ensemble size (we note that 51 members is a relatively small ensemble in the context of traditional attribution-specific experiments[43,44]), particularly for the longer, relatively less-conditioned lead times.

The focus of this study was on the attribution question, but this forecast-based methodology could be applied to produce projections designed to inform climate change adaptation. Analogous to our "future" counterfactual forecast, which we used here check the linearity of the climate change response, perturbations consistent with specific levels of global warming could be applied in order to, for example, simulate specific extreme events as if they occurred in a world of 2 °C. Such simulations of potential future extremes could be used to test the limits of regional adaptation in a targeted manner based on impactful events that have already occurred[31], complementing other approaches such as[16], which was designed to produce a rich set of different extreme events rather than specific "grey-swan" type events.

Concluding remarks In this study, we have used a numerical weather forecast-based approach to determine the contribution of human influence to a specific unprecedented extreme event. We used a state-of-the-art coupled operational weather forecast model that was unequivocally able to simulate the event in question, demonstrated by a successful prediction. Our perturbed initial condition approach maintains consistency with the measured changes in upper ocean heat content, unlike many previous approaches. We view this forecast-based approach as synthesising the storyline and probabilistic approaches to event attribution, keeping the event specificity of the storyline approach while still providing meaningful estimates of the changing risk of the extreme in question. Given that it is increasingly clear that we need to go beyond the meteorology of event attribution, and into the societal impacts[6,58], we suggest that our approach would be particularly well placed to advance this agenda, especially in the context of extremes in a future climate.

Methods

Event definition

How the extreme event of interest is quantified - the event definition - is a key methodological decision that must be made in extreme event attribution studies. A significant amount of previous work has shown the impact of the event definition on the quantitative outcome of the analysis[59,60,61]. In this study we use a definition consistent with a previous attribution study of the PNW heatwave[54] to allow for a comparison between our forecast-based approach and their probabilistic statistical and climate-model based approach.

We first average maximum temperatures over the region enclosed by 45–52N, 119–123W (indicated by the dotted rectangles in Figures 1 & 2). For the event as observed in the ERA5 reanalysis[39] we then take the peak temperature recorded during the heatwave, which occurred at 00 UTC on 2021-06-29. For the event as simulated in the medium-range forecast ensemble

members, we take the peak temperature that occurred between the 26-30th June, the period over which the heatwave occurred in reality. For the event as simulated in the seasonal forecast ensemble members, which we would not expect to predict the precise timing of the heatwave, we take the peak temperature over the full summer season. The differences between the event definitions of the medium-range and seasonal cases lead to the discrepancies in the climatologies shown in Figure 3.

Experiment details

Model details The medium-range experiments we have performed use the version of the IFS EPS that was operational at the time of the PNW heatwave, CY47R2[62]. The forecast model atmosphere is run at a resolution of O640 (18km) and has 137 vertical levels. The atmosphere is coupled to a 0.25 degree wave model[63], 0.25 degree sea ice model[64], LIM2, and 0.25 degree ocean model[65], NEMO v3.4, with 75 vertical levels (ORCA025Z75 configuration). We maintain the same number of ensemble members as the operational system, 51, throughout our experiments.

The seasonal experiments are performed with ECMWF's operational seasonal forecasting system, SEAS5[66]. This uses IFS CY43R1[67] at a horizontal resolution of Tco319 (36 km) with 91 vertical levels. The seasonal configuration of IFS CY43R1 is coupled to a 0.5 degree wave model, LIM2, and NEMO v3.4 in the ORCA025Z75 configuration. We maintain the same number of ensemble members as the operational system, 51, throughout our experiments.

Simulation setup Our experiments all use the exact operational setup (model configuration and initial conditions) as their base. To this setup, we:

1. Change the CO2 concentrations used to a "pre-industrial" level of 285 ppm, and a "future" level of 615 ppm. These represent the same fractional change in opposite directions from

the present-day concentration of 420 ppm used in the operational forecast system.

2. Subtract (for the pre-industrial forecast) or add (for the future forecast) a perturbation of the estimated anthropogenic influence on the ocean state since the pre-industrial period from the initial conditions of the forecasts (through the ocean restart files). The estimation of this perturbation is described below. We use estimated perturbations for 3D temperature, sea ice concentration, and sea ice thickness.

3. Check the sea ice fields for unphysical values. In the perturbed restarts, we ensure that sea ice concentration does not exceed 1 or subceed 0. We ensure that sea ice thickness does not subceed 0. Values outside these bounds are set to their nearest bound. Finally, we set sea ice thickness to 0 where sea ice concentration is 0, and vice versa.

4. Modify ocean salinity such that in-situ ocean density is preserved following the 3D temperature perturbation as calculated using the equation of state from the forecast ocean model. The salinity compensation is achieved to machine precision using a simple gradient descent algorithm. The resulting coupled forecasts are thermodynamically consistent with the imposed ocean heat content anomalies without any adjustments to the initial ocean circulation, mixed layer depths, or horizontal pressure gradients. Importantly, and unlike uncoupled forecasts constrained by specified sea-surface temperatures, there are no infinite sources or sinks of heat in the resulting counterfactual forecasts. This approach is justifiable in shorter-range forecasts as there is no direct influence of salinity on the overlying atmosphere. This assumption may eventually break down at lead times comparable to ocean advective processes, for which there could be indirect feedbacks on the atmosphere associated with salinity-driven changes in the ocean state. Nevertheless, this approach works well for the medium-range and seasonal forecasts described in this study.

The perturbations used are computed using an optimal fingerprint analysis[68,69,52]. We first calculate the Anthropogenic Warming Index (AWI) using anthropogenic and natural radiative forcings from AR6[70] and the HadCRUT5 global mean surface temperature dataset[71]. The AWI provides us with a plausible estimate of the fingerprint of anthropogenic influence on other climate variables[68]. For each perturbed variable, we then regress observed timeseries at each gridpoint onto the AWI, using the following data sources:

- Sea ice thickness: ORAS5 (1958:2019)[42]
- Sea ice concentration: ORAS5 (1958:2019)[42]
- Sea surface temperature: HadISSTv1.1 (1870-2019)[41]
- Subsurface temperature: WOA18 (1950-2017)[40]

We then scale the computed regression coefficients at each point by the change in AWI between the pre-industrial period of 1850-1900 and 2019 to produce our final estimated perturbations. The sea surface, and zonally and globally averaged temperature profiles are shown in Figure S1.

Finally, we combine the sea surface and subsurface temperature perturbations. We did not use a subsurface temperature dataset in isolation since observations of the sea surface temperature are considerably more abundant in the early 20th century than observations of subsurface temperatures, and since the temperatures at and near the surface are likely to be the most important for the medium-range forecasts performed, we leveraged the additional information contained in observed sea surface temperatures. We combine the two by relaxing the sea surface perturbation towards the subsurface perturbation using a relaxation depth scale of 60m (the surface autocorrelation scale in WOA18).

We note that estimation of the perturbation, and in particular the subsurface temperatures, is associated with considerable uncertainty due to the lack of observations in the pre-ARGO era. Here we have used a single best-estimate perturbation due to constraints on the available computational resource, but to account for this uncertainty an ensemble of perturbations could be applied[72]. A possible way in which such an ensemble could be derived would be to apply optimal fingerprinting to an ensemble of coupled climate models.

Bias correction of seasonal forecast ensembles

Climate drift can be an issue in the use of coupled seasonal forecast models[73]. We find a non-negligible drift in the daily maximum temperature SEAS5 forecast ensemble initialised in May over the PNW region. This drift results in a positive temperature bias that grows with lead time. Hence using the raw model output in our analysis would overestimate the probability of the PNW heatwave.

To account for the drift, we perform a simple bias-correction procedure on the seasonal forecast ensembles, informed by comparing the SEAS5 hindcasts over 1981-2020 with ERA5 reanalysis data over 1950-2020 (using the full time period that data is available and excluding the year of the event, 2021). We do this in three steps:

1. Remove the attributable forced trend from both the reanalysis and hindcasts by regressing mean JJA daily maximum temperatures onto the AWI[68].

2. Remove the drift from these detrended hindcasts, estimated by averaging the hindcasts for each lead time over all years and ensemble members, subtracting this from the corresponding reanalysis average over all years, and then regressing this timeseries onto the (linear) lead times, producing a linearly lead-time dependent drift correction[73].

3. The drift-corrected hindcasts still exhibit a positive bias during periods of extreme high

temperatures. Hence we finally remove the remaining mean bias in annual maximum temperatures in the hindcasts compared to reanalysis.

We apply this bias correction procedure to both the seasonal hindcasts shown in Figure 3 and used to estimate the return time of the event, and to the operational and perturbed seasonal forecasts of the 2021 summer. Figure S2 shows the results of this bias correction procedure, following Thompson et al.[74].

We note that validation of the bias correction procedure on the SEAS5 distribution of annual maximum temperatures (TXx) is challenging due to the unprecedented nature of the 2021 event. If we perform an analysis of the higher-order moments of the SEAS5 and "observed" (ERA5 reanalysis over 1950-2020) distributions of TXx[74], we find that the bias-corrected ensemble tends to have larger values of higher-order moments than the observed timeseries. However, if the 2021 event is included in the observed distribution, then the opposite is found, due to the large impact of such an outlier on these moments. This sensitivity to inclusion / exclusion of the 2021 event, demonstrated in Fig S2, is why we have opted to perform a simple but physically motivated bias correction rather than a more complex statistical correction such as a quantile map.

Statistical methodology

Intensity changes We calculate changes in intensity as the difference between the average of the nearest quintile of each ensemble to the event (in terms of peak temperatures). For the three longer leads, this is effectively the difference between the averages of the uppermost quintile of the two ensembles.

Risk changes We calculate the risk ratio by first fitting either a generalised extreme value (GEV) distribution to the full operational ensemble (for the shortest lead) or a straight line on a

return-time diagram (ie. an exponential tail) to the nearest quintile of either the operational ensemble (for the other two medium-range leads) or the model climatology (for the seasonal lead, since the tail of the operational ensemble lies considerably further below the event threshold than the tail of the much larger model climatology). We do this because while the shortest lead ensemble is well represented by a GEV distribution, the other three are not, and have generally heavier tails than estimated by likelihood-maximising GEV distributions. In these cases, where the event threshold lies in the extreme tail of the ensemble, the tail properties of the approximating distribution project considerably onto the estimated probability of the event. Hence to avoid any undue assumptions on the tail shape, we fit a straight line on a return-time diagram such as Figure 3 (assuming an exponential tail) to the nearest quintile.

After fitting an appropriate distribution, we then shift the location of this distribution by the estimated attributable warming. We then calculate the probability of observing an event at least as intense as the PNW heatwave (the dashed line in Figure 3) in the original distribution and the shifted distribution. The risk ratio is the ratio of these two probabilities (Pcurrent / Pshifted).

Throughout, confidence intervals are calculated using a 10,000 member non-parametric bootstrap with replacement.

References

[1] National Academies of Sciences, a. M., Engineering. *Attribution of Extreme Weather Events in the Context of Climate Change* (National Academies Press, Washington, D.C., 2016). URL `https://nap.nationalacademies.org/catalog/21852/attribution-of-extreme-weather-events-in-the-context-of-climate-change`

[2] White, R. *et al.* The Unprecedented Pacific Northwest Heatwave of June 2021. *na-*

ture portfolio **under review** (2022). URL https://doi.org/10.21203/rs.3.rs-1520351/v1.

[3] Shepherd, T. G. A Common Framework for Approaches to Extreme Event Attribution. *Curr Clim Change Rep* **2**, 28–38 (2016).

[4] Stott, P. A., Stone, D. A. & Allen, M. R. Human contribution to the European heatwave of 2003. *Nature* **432**, 610–614 (2004). URL http://www.nature.com/articles/nature03089. Publisher: Nature Publishing Group.

[5] Harrington, L. J., Ebi, K. L., Frame, D. J. & Otto, F. E. L. Integrating attribution with adaptation for unprecedented future heatwaves. *Climatic Change* **172**, 1–7 (2022). URL https://link.springer.com/article/10.1007/s10584-022-03357-4. Company: Springer Distributor: Springer Institution: Springer Label: Springer Number: 1 Publisher: Springer Netherlands.

[6] Mitchell, D. Climate attribution of heat mortality. *Nature Climate Change* **11**, 467–468 (2021). URL https://www.nature.com/articles/s41558-021-01049-y. Number: 6 Publisher: Nature Publishing Group.

[7] Trenberth, K. E., Fasullo, J. T. & Shepherd, T. G. Attribution of climate extreme events. *Nature Climate Change* **5**, 725–730 (2015). URL http://www.nature.com/articles/nclimate2657. Publisher: Nature Publishing Group.

[8] Hoerling, M. *et al.* Anatomy of an extreme event. *Journal of Climate* **26**, 2811–2832 (2013). URL http://journals.ametsoc.org/jcli/article-pdf/26/9/2811/4013161/jcli-d-12-00270_1.pdf. Publisher: American Meteorological Society.

[9] Philip, S. *et al.* A protocol for probabilistic extreme event attribution analyses. *Advances in Statistical Climatology, Meteorology and Oceanography* **6**, 177–203 (2020). URL https://ascmo.copernicus.org/articles/6/177/2020/.

[10] Pall, P. *et al.* Anthropogenic greenhouse gas contribution to flood risk in England and Wales in autumn 2000. *Nature* **470**, 382–385 (2011). URL http://www.nature.com/articles/nature09762.

[11] Van Oldenborgh, G. J. How unusual was autumn 2006 in Europe? *Climate of the Past* **3**, 659–668 (2007). URL https://cp.copernicus.org/articles/3/659/2007/. Publisher: Copernicus GmbH.

[12] Gessner, C., Fischer, E. M., Beyerle, U. & Knutti, R. Very Rare Heat Extremes: Quantifying and Understanding Using Ensemble Reinitialization. *Journal of Climate* **34**, 6619–6634 (2021). URL https://journals.ametsoc.org/view/journals/clim/aop/JCLI-D-20-0916.1/JCLI-D-20-0916.1.xml. Publisher: American Meteorological Society Section: Journal of Climate.

[13] Masato, G., Hoskins, B. J. & Woollings, T. Winter and Summer Northern Hemisphere Blocking in CMIP5 Models. *Journal of Climate* **26**, 7044–7059 (2013). URL https://journals.ametsoc.org/view/journals/clim/26/18/jcli-d-12-00466.1.xml. Publisher: American Meteorological Society Section: Journal of Climate.

[14] Payne, A. E. & Magnusdottir, G. An evaluation of atmospheric rivers over the North Pacific in CMIP5 and their response to warming under RCP 8.5. *Journal of Geophysical Research: Atmospheres* **120**, 11,173–11,190 (2015). URL https://

onlinelibrary.wiley.com/doi/abs/10.1002/2015JD023586. _eprint: https://onlinelibrary.wiley.com/doi/pdf/10.1002/2015JD023586.

[15] Fischer, E. M., Sippel, S. & Knutti, R. Increasing probability of record-shattering climate extremes. *Nature Climate Change* 1–7 (2021). URL https://www.nature.com/articles/s41558-021-01092-9. Bandiera_abtest: a Cg_type: Nature Research Journals Primary_atype: Research Publisher: Nature Publishing Group Subject_term: Climate and Earth system modelling;Projection and prediction Subject_term_id: climate-and-earth-system-modelling;projection-and-prediction.

[16] Leach, N. J., Watson, P. A. G., Sparrow, S. N., Wallom, D. C. H. & Sexton, D. M. H. Generating samples of extreme winters to support climate adaptation. *Weather and Climate Extremes* **36**, 100419 (2022). URL https://www.sciencedirect.com/science/article/pii/S2212094722000111.

[17] Palmer, T. N. A Nonlinear Dynamical Perspective on Climate Prediction. *Journal of Climate* **12**, 575–591 (1999). URL https://journals.ametsoc.org/view/journals/clim/12/2/1520-0442_1999_012_0575_andpoc_2.0.co_2.xml. Publisher: American Meteorological Society Section: Journal of Climate.

[18] Palmer, T. N. & Weisheimer, A. A SIMPLE PEDAGOGICAL MODEL LINKING INITIAL-VALUE RELIABILITY WITH TRUSTWORTHINESS IN THE FORCED CLIMATE RESPONSE. *Bulletin of the American Meteorological Society* **99**, 605–614 (2018). URL http://journals.ametsoc.org/doi/10.1175/BAMS-D-16-0240.1. Publisher: American Meteorological Society.

[19] Van Garderen, L., Feser, F. & Shepherd, T. G. A methodology for attributing the role of

climate change in extreme events: A global spectrally nudged storyline. *Natural Hazards and Earth System Sciences* **21**, 171–186 (2021). Publisher: Copernicus GmbH.

[20] Benítez, A. S., Goessling, H., Pithan, F., Semmler, T. & Jung, T. The July 2019 European heatwave in a warmer climate: Storyline scenarios with a coupled model using spectral nudging. *Journal of Climate* **-1**, 1–51 (2022). URL https://journals.ametsoc.org/view/journals/clim/aop/JCLI-D-21-0573.1/JCLI-D-21-0573.1.xml. Publisher: American Meteorological Society Section: Journal of Climate.

[21] Leach, N. J., Weisheimer, A., Allen, M. R. & Palmer, T. Forecast-based attribution of a winter heatwave within the limit of predictability. *Proceedings of the National Academy of Sciences* **118** (2021). URL https://ezproxy-prd.bodleian.ox.ac.uk:3006/content/118/49/e2112087118. ISBN: 9782112087117 Publisher: National Academy of Sciences Section: Physical Sciences.

[22] Roberts, C. D. *et al.* Climate model configurations of the ECMWF Integrated Forecasting System (ECMWF-IFS cycle 43r1) for HighResMIP. *Geoscientific Model Development* **11**, 3681–3712 (2018). URL https://gmd.copernicus.org/articles/11/3681/2018/. Publisher: Copernicus GmbH.

[23] Hope, P., Lim, E.-P., Wang, G., Hendon, H. H. & Arblaster, J. M. Contributors to the Record High Temperatures Across Australia in Late Spring 2014. *Bulletin of the American Meteorological Society* **96**, S149–S153 (2015). URL https://journals.ametsoc.org/view/journals/bams/96/12/bams-d-15-00096.1.xml. Publisher: American Meteorological Society Section: Bulletin of the American Meteorological Society.

[24] Hope, P., Wang, G., Lim, E.-P., Hendon, H. H. & Arblaster, J. M. What Caused the Record-Breaking Heat Across Australia in October 2015? *Bulletin of the American Meteorological Society* **97**, S122–S126 (2016). URL https://journals.ametsoc.org/view/journals/bams/97/12/bams-d-16-0141.1.xml. Publisher: American Meteorological Society Section: Bulletin of the American Meteorological Society.

[25] Hope, P. *et al.* On Determining the Impact of Increasing Atmospheric CO2 on the Record Fire Weather in Eastern Australia in February 2017. *Bulletin of the American Meteorological Society* **100**, S111–S117 (2019). URL https://journals.ametsoc.org/view/journals/bams/100/1/bams-d-18-0135.1.xml. Publisher: American Meteorological Society Section: Bulletin of the American Meteorological Society.

[26] Wang, G., Hope, P., Lim, E.-P., Hendon, H. H. & Arblaster, J. M. An Initialized Attribution Method for Extreme Events on Subseasonal to Seasonal Time Scales. *Journal of Climate* **34**, 1453–1465 (2021). URL https://journals.ametsoc.org/view/journals/clim/aop/JCLI-D-19-1021.1/JCLI-D-19-1021.1.xml. Publisher: American Meteorological Society Section: Journal of Climate.

[27] Hope, P. *et al.* Subseasonal to Seasonal Climate Forecasts Provide the Backbone of a Near-Real-Time Event Explainer Service. *Bulletin of the American Meteorological Society* **103**, S7–S13 (2022). URL https://journals.ametsoc.org/view/journals/bams/103/3/BAMS-D-21-0253.1.xml. Num Pages: 7 Number: 3 Place: United States Publisher: American Meteorological Society.

[28] Pall, P. *et al.* Diagnosing conditional anthropogenic contributions to heavy Colorado rainfall in September 2013. *Weather and Climate Extremes* **17**, 1–6 (2017). Publisher: Elsevier B.V.

[29] Wehner, M. F., Zarzycki, C. & Patricola, C. Estimating the Human Influence on Tropical Cyclone Intensity as the Climate Changes. In Collins, J. M. & Walsh, K. (eds.) *Hurricane Risk*, Hurricane Risk, 235–260 (Springer International Publishing, Cham, 2019). URL https://doi.org/10.1007/978-3-030-02402-4_12.

[30] Tradowsky, J. S. *et al.* Toward Near-Real-Time Attribution of Extreme Weather Events in Aotearoa New Zealand. *Bulletin of the American Meteorological Society* **103**, S105–S110 (2022). URL https://journals.ametsoc.org/view/journals/bams/103/3/BAMS-D-21-0236.1.xml. Publisher: American Meteorological Society Section: Bulletin of the American Meteorological Society.

[31] Hazeleger, W. *et al.* Tales of future weather. *NATURE CLIMATE CHANGE* **5** (2015).

[32] Henderson, S. B., McLean, K. E., Lee, M. J. & Kosatsky, T. Analysis of community deaths during the catastrophic 2021 heat dome: Early evidence to inform the public health response during subsequent events in greater Vancouver, Canada. *Environmental Epidemiology* **6**, e189 (2022). URL https://journals.lww.com/environepidem/Fulltext/2022/02000/Analysis_of_community_deaths_during_the.8.aspx.

[33] Menne, M. J. *et al.* Global Historical Climatology Network - Daily (GHCN-Daily), Version 3.26 (2012). URL https://gis.ncdc.noaa.gov/geoportal/catalog/search/resource/details.page?id=gov.noaa.ncdc:C00861. Publication Title: NOAA National Climate Data Center.

[34] Menne, M. J., Durre, I., Vose, R. S., Gleason, B. E. & Houston, T. G. An Overview of the Global Historical Climatology Network-Daily Database. *Journal of Atmospheric and*

Oceanic Technology **29**, 897–910 (2012). URL http://journals.ametsoc.org/doi/10.1175/JTECH-D-11-00103.1.

[35] Overland, J. E. Causes of the Record-Breaking Pacific Northwest Heatwave, Late June 2021. *Atmosphere* **12**, 1434 (2021). URL https://www.mdpi.com/2073-4433/12/11/1434. Number: 11 Publisher: Multidisciplinary Digital Publishing Institute.

[36] Lin, H., Mo, R. & Vitart, F. The 2021 Western North American Heatwave and Its Subseasonal Predictions. *Geophysical Research Letters* **49**, e2021GL097036 (2022). URL https://onlinelibrary.wiley.com/doi/abs/10.1029/2021GL097036. _eprint: https://onlinelibrary.wiley.com/doi/pdf/10.1029/2021GL097036.

[37] Mo, R., Lin, H. & Vitart, F. An anomalous warm-season trans-Pacific atmospheric river linked to the 2021 western North America heatwave. *Communications Earth & Environment* **3**, 1–12 (2022). URL https://www.nature.com/articles/s43247-022-00459-w. Number: 1 Publisher: Nature Publishing Group.

[38] Thompson, V. *et al.* The 2021 western North America heat wave among the most extreme events ever recorded globally. *Science Advances* **8**, eabm6860 (2022). URL https://www.science.org/doi/10.1126/sciadv.abm6860. Publisher: American Association for the Advancement of Science.

[39] Hersbach, H. *et al.* The ERA5 global reanalysis. *Quarterly Journal of the Royal Meteorological Society* **146**, 1999–2049 (2020). URL https://onlinelibrary.wiley.com/doi/abs/10.1002/qj.3803. Publisher: John Wiley & Sons, Ltd.

[40] Locarnini, R. A. *et al.* World Ocean Atlas 2018, Volume 1: Temperature. Tech. Rep. 82,

NOAA National Centers for Environmental Information (2019). A. Mishonov Technical Ed.

[41] Rayner, N. A. *et al.* Global analyses of sea surface temperature, sea ice, and night marine air temperature since the late nineteenth century. *Journal of Geophysical Research* **108**, 4407 (2003). URL http://doi.wiley.com/10.1029/2002JD002670. Publisher: John Wiley & Sons, Ltd.

[42] Zuo, H., Balmaseda, M. A., Tietsche, S., Mogensen, K. & Mayer, M. The ECMWF operational ensemble reanalysis–analysis system for ocean and sea ice: a description of the system and assessment. *Ocean Science* **15**, 779–808 (2019). URL https://os.copernicus.org/articles/15/779/2019/. Publisher: Copernicus GmbH.

[43] Massey, N. *et al.* weather@home-development and validation of a very large ensemble modelling system for probabilistic event attribution. *Quarterly Journal of the Royal Meteorological Society* **141**, 1528–1545 (2015). URL http://doi.wiley.com/10.1002/qj.2455. Publisher: John Wiley & Sons, Ltd.

[44] Ciavarella, A. *et al.* Upgrade of the HadGEM3-A based attribution system to high resolution and a new validation framework for probabilistic event attribution. *Weather and Climate Extremes* **20**, 9–32 (2018). URL https://www.sciencedirect.com/science/article/pii/S2212094717301305. Publisher: Elsevier.

[45] Douville, H. *et al.* Water Cycle Changes. In Masson-Delmotte, V. *et al.* (eds.) *Climate Change 2021: The Physical Science Basis. Contribution of Working Group I to the Sixth Assessment Report of the Intergovernmental Panel on Climate Change*, 1055–1210 (Cambridge University Press, Cambridge, United Kingdom and New York, NY, USA, 2021).

[46] Gulev, S. *et al.* Changing State of the Climate System. In Masson-Delmotte, V. *et al.* (eds.) *Climate Change 2021: The Physical Science Basis. Contribution of Working Group I to the Sixth Assessment Report of the Intergovernmental Panel on Climate Change*, 287–422 (Cambridge University Press, Cambridge, United Kingdom and New York, NY, USA, 2021).

[47] Gutiérrez, J. *et al.* Atlas. In Masson-Delmotte, V. *et al.* (eds.) *Climate Change 2021: The Physical Science Basis. Contribution of Working Group I to the Sixth Assessment Report of the Intergovernmental Panel on Climate Change*, 1927–2058 (Cambridge University Press, Cambridge, United Kingdom and New York, NY, USA, 2021).

[48] Christidis, N. & Stott, P. A. Changes in the geopotential height at 500 hPa under the influence of external climatic forcings. *Geophysical Research Letters* **42**, 10,798–10,806 (2015). URL https://agupubs.onlinelibrary.wiley.com/doi/abs/10.1002/2015GL066669. _eprint: https://agupubs.onlinelibrary.wiley.com/doi/pdf/10.1002/2015GL066669.

[49] Allen, M. R. & Ingram, W. J. Constraints on future changes in climate and the hydrologic cycle. *Nature* **419**, 228–232 (2002). URL https://www.nature.com/articles/nature01092. Number: 6903 Publisher: Nature Publishing Group.

[50] Seneviratne, S. I. & Hauser, M. Regional Climate Sensitivity of Climate Extremes in CMIP6 Versus CMIP5 Multimodel Ensembles. *Earth's Future* **8**, e2019EF001474 (2020). URL https://onlinelibrary.wiley.com/doi/abs/10.1029/2019EF001474. _eprint: https://onlinelibrary.wiley.com/doi/pdf/10.1029/2019EF001474.

[51] Osborn, T. J. *et al.* Land Surface Air Temperature Variations Across the

Globe Updated to 2019: The CRUTEM5 Data Set. *Journal of Geophysical Research: Atmospheres* **126**, e2019JD032352 (2021). URL https://onlinelibrary.wiley.com/doi/abs/10.1029/2019JD032352. _eprint: https://onlinelibrary.wiley.com/doi/pdf/10.1029/2019JD032352.

[52] Haustein, K. *et al.* A real-time Global Warming Index. *Scientific Reports* **7**, 15417 (2017). URL http://www.nature.com/articles/s41598-017-14828-5. Publisher: Nature Publishing Group.

[53] Stone, D. A. & Allen, M. R. The end-to-end attribution problem: From emissions to impacts. *Climatic Change* **71**, 303–318 (2005). Publisher: Springer.

[54] Philip, S. Y. *et al.* Rapid attribution analysis of the extraordinary heatwave on the Pacific Coast of the US and Canada June 2021. *Earth System Dynamics Discussions* 1–34 (2021). URL https://esd.copernicus.org/preprints/esd-2021-90/. Publisher: Copernicus GmbH.

[55] Fischer, E. M., Seneviratne, S. I., Lüthi, D. & Schär, C. Contribution of land-atmosphere coupling to recent European summer heat waves. *Geophysical Research Letters* **34** (2007). URL https://agupubs.onlinelibrary.wiley.com/doi/10.1029/2006GL029068. Publisher: John Wiley & Sons, Ltd.

[56] Wehner, M. F. & Reed, K. A. Operational extreme weather event attribution can quantify climate change loss and damages. *PLOS Climate* **1**, e0000013 (2022). URL https://journals.plos.org/climate/article?id=10.1371/journal.pclm.0000013. Publisher: Public Library of Science.

[57] Reed, K. A., Wehner, M. F. & Zarzycki, C. M. Attribution of 2020 hurricane season extreme rainfall to human-induced climate change. *Nature Communications* **13**, 1905

(2022). URL https://www.nature.com/articles/s41467-022-29379-1. Number: 1 Publisher: Nature Publishing Group.

[58] Mitchell, D. *et al.* Increased population exposure to Amphan-scale cyclones under future climates. *Climate Resilience and Sustainability* **1**, e36 (2022). URL https://onlinelibrary.wiley.com/doi/abs/10.1002/cli2.36. _eprint: https://onlinelibrary.wiley.com/doi/pdf/10.1002/cli2.36.

[59] Uhe, P. *et al.* Comparison of methods: Attributing the 2014 record European temperatures to human influences. *Geophysical Research Letters* **43**, 8685–8693 (2016). URL http://doi.wiley.com/10.1002/2016GL069568. Publisher: John Wiley & Sons, Ltd.

[60] Kirchmeier-Young, M. C., Wan, H., Zhang, X. & Seneviratne, S. I. Importance of Framing for Extreme Event Attribution: The Role of Spatial and Temporal Scales. *Earth's Future* **7**, 1192–1204 (2019). URL https://onlinelibrary.wiley.com/doi/abs/10.1029/2019EF001253. Publisher: American Geophysical Union (AGU).

[61] Angélil, O. *et al.* On the nonlinearity of spatial scales in extreme weather attribution statements. *Climate Dynamics* **50**, 2739–2752 (2018). Publisher: Springer Verlag.

[62] *IFS Documentation CY47R2*. IFS Documentation (ECMWF, 2020). URL https://www.ecmwf.int/. DOIs: http://dx.doi.org/10.21957/ftq7iq93j http://dx.doi.org/10.21957/0gtybbwp9 http://dx.doi.org/10.21957/u8ssd58 http://dx.doi.org/10.21957/cpmkqvhja http://dx.doi.org/10.21957/d7e3hrb http://dx.doi.org/10.21957/56v1qbf0n http://dx.doi.org/10.21957/31drbygag.

[63] Janssen, P. *The Interaction of Ocean Waves and Wind* (Cambridge University Press, Cambridge, 2004). URL https://www.cambridge.

org/core/books/interaction-of-ocean-waves-and-wind/7C73904891BAFD83F27A9EA2E09A6E50.

[64] Fichefet, T. & Maqueda, M. A. M. Sensitivity of a global sea ice model to the treatment of ice thermodynamics and dynamics. *Journal of Geophysical Research: Oceans* **102**, 12609–12646 (1997). URL https://onlinelibrary.wiley.com/doi/abs/10.1029/97JC00480. _eprint: https://onlinelibrary.wiley.com/doi/pdf/10.1029/97JC00480.

[65] Madec, G. NEMO ocean engine. Project Report, Institut Pierre-Simon Laplace (IPSL) (2008). URL https://eprints.soton.ac.uk/64324/. Series: 27.

[66] Johnson, S. J. *et al.* SEAS5: The new ECMWF seasonal forecast system. *Geoscientific Model Development* **12**, 1087–1117 (2019). URL https://www.geosci-model-dev.net/12/1087/2019/. Publisher: Copernicus GmbH.

[67] *IFS Documentation CY43R1*. IFS Documentation (ECMWF, 2016). URL https://www.ecmwf.int/. DOIs: http://dx.doi.org/10.21957/7zo03h0ve http://dx.doi.org/10.21957/am5dtg9pb http://dx.doi.org/10.21957/m1u2yxwrl http://dx.doi.org/10.21957/sqvo5yxja http://dx.doi.org/10.21957/6fm80smm http://dx.doi.org/10.21957/xc3eo8i41 http://dx.doi.org/10.21957/18mel2ooj.

[68] Hasselmann, K. Optimal Fingerprints for the Detection of Time-dependent Climate Change. *Journal of Climate* **6**, 1957–1971 (1993). URL https://journals.ametsoc.org/view/journals/clim/6/10/1520-0442_1993_006_1957_offtdo_2_0_co_2.xml. Publisher: American Meteorological Society Section: Journal of Climate.

[69] Hasselmann, K. Multi-pattern fingerprint method for detection and attribution of climate change. *Climate Dynamics* **13**, 601–611 (1997). URL http://link.springer.com/10.1007/s003820050185. Publisher: Springer-Verlag.

[70] Forster, P. *et al.* The Earth's Energy Budget, Climate Feedbacks, and Climate Sensitivity. In Masson-Delmotte, V. *et al.* (eds.) *Climate Change 2021: The Physical Science Basis. Contribution of Working Group I to the Sixth Assessment Report of the Intergovernmental Panel on Climate Change*, 923–1054 (Cambridge University Press, Cambridge, United Kingdom and New York, NY, USA, 2021).

[71] Morice, C. P. *et al.* An Updated Assessment of Near-Surface Temperature Change From 1850: The HadCRUT5 Data Set. *Journal of Geophysical Research: Atmospheres* **126** (2021). URL https://onlinelibrary.wiley.com/doi/10.1029/2019JD032361. Publisher: John Wiley & Sons, Ltd.

[72] Sparrow, S. *et al.* Attributing human influence on the July 2017 Chinese heatwave: the influence of sea-surface temperatures. *Environ. Res. Lett* **13**, 114004 (2018). URL https://doi.org/10.1088/1748-9326/aae356.

[73] Stockdale, T. N. Coupled Ocean–Atmosphere Forecasts in the Presence of Climate Drift. *Monthly Weather Review* **125**, 809–818 (1997). URL https://journals.ametsoc.org/view/journals/mwre/125/5/1520-0493_1997_125_0809_coafit_2.0.co_2.xml. Publisher: American Meteorological Society Section: Monthly Weather Review.

[74] Thompson, V. *et al.* High risk of unprecedented UK rainfall in the current climate. *Nature Communications* **8**, 1–6 (2017). URL www.nature.com/naturecommunications. Publisher: Nature Publishing Group.

Acknowledgments

We thank Paul Dando, Robin Hogan and Andrew Dawson for their help with setting up IFS for our experiments. The results contain modified Copernicus Climate Change Service information [2022]. Neither the European Commission nor ECMWF is responsible for any use that may be made of the Copernicus information or data it contains. N.J.L. was supported by the Natural Environment Research Council under Grant NE/L002612/1. A.W. was supported by the European Union's Horizon 2020 project European Climate Predictions (EUCP) under Grant GA 776613. M.R.A. was supported by the European Union's Horizon 2020 project FORCeS under Grant GA 821205. Acknowledgement is made for the use of ECMWF's computing and archive facilities in this research under the special project *spgbleac*.

Supplementary materials

Figs. S1 to S7

Supplementary Files

This is a list of supplementary files associated with this preprint. Click to download.

- leachetal22SI.pdf